Three-equation model for the self-similar growth of Rayleigh-Taylor and Richtmyer-Meskov instabilities

Brandon E. Morgan and Michael E. Wickett

Phys. Rev. E **91**, 043002 — Published 6 April 2015

DOI: 10.1103/PhysRevE.91.043002

Three-equation model for the self-similar growth of Rayleigh-Taylor and Richtmyer-Meskov instabilities

Brandon E. Morgan and Michael E. Wickett
Lawrence Livermore National Laboratory
Livermore, California 94550

In the present work, the two-equation k-L model [G. Dimonte and R. Tipton, "K-L turbulence model for the self-similar growth of the Rayleigh-Taylor and Richtmyer-Meshkov instabilities," Phys. Fluids **18** (2006)] is extended by the addition of a third equation for the mass-flux velocity. A set of model constants is derived to satisfy an ansatz of self-similarity in the low Atwood number limit. The model is then applied to the simulation of canonical Rayleigh-Taylor and Richtmyer-Meshkov test problems in one dimension and is demonstrated to reproduce analytical self-similar growth and to recover growth rates used to constrain the model.

Keywords: turbulent mixing, turbulence modeling, Rayleigh-Taylor, Richtmyer-Meshkov

I. INTRODUCTION

The k-L model [1] is a two-equation Reynolds-Averaged Navier-Stokes (RANS) model developed specifically for its application to the prediction of Rayleigh-Taylor (RT) and Richtmyer-Meshkov (RM) instabilities. Since its development, the k-L model has been demonstrated to provide good agreement with theoretical growth rates of RT- and RM-induced mixing [1, 2] and has been applied to a wide range of applications including prediction of astrophysical phenomena [3] and simulation of inertial confinement fusion (ICF) targets [4]. To close the pressure work term in the turbulence kinetic energy equation (sometimes referred to as the *buoyancy source* or *buoyancy production* term), the k-L model relies on a gradient diffusion approximation to model the mass-flux velocity, a_i. Of course, it is expected that such an approximation should break down for flows with significant counter-gradient transport [5]. An alternative approach which is utilized by the Besnard-Harlow-Rauenzen (BHR) family of models [6–8] is to instead solve a transport equation for the mass-flux velocity.

One common issue that often arises in RANS model development is the determination of certain model constants that appear as scaling coefficients on turbulence closures. In the BHR family of models, separate sets of model constants are prescribed for the simulation of RT and RM flows [7, 8]. For complex flows which may involve combined fluid instabilities, such an approach is likely to be unsatisfactory. It is therefore desirable to develop a single model which may be applied consistently in the prediction of both RT- and RM-type flows. In the present work, an extension to the traditional k-L model is presented with the addition of a transport equation for a_i (henceforward referred to as the k-L-a model). Similarity analysis used by Dimonte and Tipton [1] to determine k-L model constants is then extended to encompass the a_i equation, and constraints on model constants are derived based on expected self-similar growth rates for RT and RM flows. Later, the expected self-similar growth is confirmed through application of the k-L-a model to the simulation of RT and RM flows in one dimension.

II. THE k-L-a MODEL EQUATIONS

The k-L-a RANS model is derived from the compressible Navier-Stokes equations for a multi-component, non-reactive gas mixture. In the present work, an overbar is used to denote Reynolds averaging, and a tilde is used to denote mass-weighted (Favre) averaging. Decomposition of an arbitrary scalar, f, may therefore be written

$$f = \overline{f} + f' = \widetilde{f} + f'' \tag{1}$$

where the Favre average is related to the Reynolds average through the density, ρ, according to

$$\widetilde{f} = \frac{\overline{\rho f}}{\overline{\rho}} \,. \tag{2}$$

Utilizing this notation, we introduce the Reynolds stress tensor, τ_{ij}, the mass-flux velocity vector, a_i, and the density-specific-volume correlation, b, in terms of the velocity vector, u_i, and the specific volume, $v \equiv 1/\rho$

$$\overline{\rho}\tau_{ij} \equiv -\overline{\rho u_i'' u_j''} \tag{3a}$$

$$a_i \equiv -\overline{u_i''} \tag{3b}$$

$$b \equiv -\overline{\rho' v'} \,. \tag{3c}$$

Equations 4 through 10 summarize the model. In these equations, t is time; x_i is the spatial dimension vector; g_i is the gravitational acceleration vector; p is static pressure; e is the specific internal energy; Y_α is the scalar mass fraction of component α; k is the turbulence kinetic energy; L is the turbulence lengthscale; and μ_t is an eddy viscosity. b is closed in equation 13 in terms of component partial densities, ρ_α, and volume fractions, V_α. C_μ, C_a, C_B, C_D, C_L, N_a, N_e, N_k, N_L, N_Y, and c are undetermined model constants which will be set through

similarity analysis. C_{dev} is a multiplier on the deviatoric component of the Reynolds stress. For now, we follow the approach of Sinha *et al.* [9] by setting $C_{dev} = 0$ to avoid pathological over-amplification of turbulence in the presence of shocks.

$$\frac{D\overline{\rho}}{Dt} = -\overline{\rho}\frac{\partial \widetilde{u}_i}{\partial x_i} \tag{4}$$

$$\overline{\rho}\frac{D\widetilde{Y}_\alpha}{Dt} = \frac{\partial}{\partial x_i}\left(\frac{\mu_t}{N_Y}\frac{\partial \widetilde{Y}_\alpha}{\partial x_i}\right) \tag{5}$$

$$\overline{\rho}\frac{D\widetilde{u}_j}{Dt} = -\frac{\partial \overline{p}}{\partial x_j} + \frac{\partial}{\partial x_i}\left(\overline{\rho}\tau_{ij}\right) + \overline{\rho}g_j \tag{6}$$

$$\begin{aligned}\overline{\rho}\frac{D\widetilde{e}}{Dt} =& -\overline{p}\frac{\partial \widetilde{u}_i}{\partial x_i} - a_j\frac{\partial \overline{p}}{\partial x_i} + C_D\frac{\overline{\rho}\left(2k\right)^{3/2}}{L} \\ &+ \frac{\partial}{\partial x_j}\left(\frac{\mu_t}{N_e}\frac{\partial \widetilde{e}}{\partial x_j}\right)\end{aligned} \tag{7}$$

$$\begin{aligned}\overline{\rho}\frac{Dk}{Dt} =& \overline{\rho}\tau_{ij}\frac{\partial \widetilde{u}_i}{\partial x_j} + a_j\frac{\partial \overline{p}}{\partial x_i} - C_D\frac{\overline{\rho}\left(2k\right)^{3/2}}{L} \\ &+ \frac{\partial}{\partial x_i}\left(\frac{\mu_t}{N_k}\frac{\partial k}{\partial x_i}\right)\end{aligned} \tag{8}$$

$$\overline{\rho}\frac{DL}{Dt} = \frac{1}{3}\overline{\rho}L\frac{\partial \widetilde{u}_i}{\partial x_i} + C_L\overline{\rho}\sqrt{2k} + \frac{\partial}{\partial x_i}\left(\frac{\mu_t}{N_L}\frac{\partial L}{\partial x_i}\right) \tag{9}$$

$$\begin{aligned}\overline{\rho}\frac{Da_j}{Dt} =& C_B^2 b\frac{\partial \overline{p}}{\partial x_j} - C_a\overline{\rho}a_j\frac{\left(2k\right)^{1/2}}{L} + \tau_{ij}\frac{\partial \overline{\rho}}{\partial x_i} \\ &+ \frac{\partial}{\partial x_i}\left(\frac{\mu_t}{N_a}\frac{\partial a_j}{\partial x_i}\right)\end{aligned} \tag{10}$$

where

$$\frac{D}{Dt} \equiv \frac{\partial}{\partial t} + \widetilde{u}_i\frac{\partial}{\partial x_i} \tag{11}$$

$$\mu_t = C_\mu\overline{\rho}L\sqrt{2k} \tag{12}$$

$$b = \overline{\rho}\left(\frac{\sum_\alpha \frac{V_\alpha}{\rho_\alpha + c\overline{\rho}}}{\sum_\alpha \frac{V_\alpha\rho_\alpha}{\rho_\alpha + c\overline{\rho}}}\right) - 1 \tag{13}$$

$$\overline{S}_{ij} = \frac{1}{2}\left(\frac{\partial \widetilde{u}_i}{\partial x_j} + \frac{\partial \widetilde{u}_j}{\partial x_i}\right) - \frac{1}{3}\frac{\partial \widetilde{u}_k}{\partial x_k}\delta_{ij} \tag{14}$$

$$\overline{\rho}\tau_{ij} = C_{dev}\left(2\mu_t\overline{S}_{ij}\right) - \frac{2}{3}\overline{\rho}k\delta_{ij}\,. \tag{15}$$

Although addition of an equation for the mass-flux velocity is similar to (and indeed inspired by) the BHR k-S-a model [7], our approach in the present work is to start with the 2006 Dimonte and Tipton model [1] and to extend it in such a way that additional model constants may be closed through similarity analysis. Although Banerjee *et al.* [7] have utilized limited similarity analysis of a low-Atwood number RT flow to constrain a subset of parameters in the k-S-a model, the present approach is to apply similarity analysis in a broader sense to all model constants, limiting parameterization to a few experimentally observable characteristics of RT and RM flow as Dimonte and Tipton have done for the 2006 k-L model [1]. As a result, the present model differs from the BHR k-S-a model in the following ways: firstly, production terms that scale like L/k are neglected in the transport equation for L as these terms and do not appear in the 2006 model, and they can be sensitive to unphysical transient oscillations when appearing in concert with terms scaling like k/L (as in the e, k, and a equations). Secondly, only shear and Reynolds stress production terms are included in the a_i equation, as the additional production terms which appear in the BHR k-S-a model are generally small for RM and RT flows [8]. Additionally, in the present model, closure for the velocity-pressure gradient correlation in the internal energy equation is chosen to exactly equal the buoyancy production term in the k equation; this choice again derives from the 2006 k-L model and imposes a symmetric exchange between turbulence kinetic energy and internal energy. Finally, the algebraic closure for b in the present model is generalized for an n-component mixture and includes an added-mass correction factor, c.

III. SIMILARITY ANALYSIS

We now utilize an ansatz of self-similarity to determine values for the model constants listed in the previous section. Constants are chosen to satisfy the self-similarity ansatz and reproduce the expected self-similar growth of one-dimensional RT- and RM-induced mixing layers. In this section, the overbar notation to indicate Reynolds-average quantities is dropped for simplicity yet remains implied. Analysis is further simplified by assumptions of incompressible flow at low Atwood number. These approximations together allow us to drop spatial derivatives of velocity and to divide out factors of $\overline{\rho}$. Mean convective terms arising from the material derivative and the second production term in the L equation, $\overline{\rho}L\frac{\partial \widetilde{u}_i}{\partial x_j}$, are therefore not included in the similarity analysis; a model coefficient of 1/3 is assumed for the second L production term based on the original argument of mass conservation under compression given by Dimonte and Tipton [1].

A. Self-Similarity of the L Equation

To begin, a change of variable is introduced in terms of the self-similar mixing width, $h(t)$. Let $\chi \equiv x/h$. It is then assumed that the analytic functions k and L are separable in space and time such that $k(\chi,t) = K_0(t)f(\chi)$ and $L(\chi,t) = L_0(t)f^{1/2}(\chi)$. By applying the simplifying assumptions and substituting into equation 9, the one-dimensional L equation can be reduced to

$$\begin{aligned}\frac{D}{Dt}\left(L_0 f^{1/2}\right) =& \frac{\partial}{\partial x}\left[\frac{C_\mu}{N_L} L_0 f \sqrt{2K_0}\frac{\partial}{\partial x}\left(L_0 f^{1/2}\right)\right] \\ &+ C_L f^{1/2}\sqrt{2K_0}\,. \end{aligned} \tag{16}$$

The self-similarity ansatz is then applied by assuming that the spatial function f is self-similar such that $f(\chi) = 1-\chi^2$ and $L_0(t) = \beta h(t)$. Equation 16 is then transformed further to equation 17, where a dot indicates differentiation with respect to time.

$$\begin{aligned}\dot{L}_0 =& \sqrt{2K_0}\left(C_L - \frac{C_\mu}{N_L}\beta^2\right) \\ &+ \sqrt{2K_0}\left(2\frac{C_\mu}{N_L}\beta^2 - C_L\right)\left(\frac{x}{h}\right)^2 . \end{aligned} \tag{17}$$

In order to satisfy the self-similarity ansatz, equation 17 must be satisfied for all x. Since the left-hand side is a function of time only, it is required that the terms proportional to x^2 must vanish. This requirement is satisfied if $\beta = \left[C_L N_L/(2C_\mu)\right]^{1/2}$. Inserting this constraint back into equation 17 then gives

$$\dot{L}_0(t) = \frac{C_L}{2}\sqrt{2K_0}\,. \tag{18}$$

B. Self-Similarity of the a Equation

Consider an RT-unstable configuration of two fluids in hydrostatic equilibrium with gravitational acceleration. This permits transformation of equation 10 to

$$\begin{aligned}\rho\frac{Da}{Dt} =& \frac{\partial}{\partial x}\left(\frac{\mu_t}{N_a}\frac{\partial a}{\partial x}\right) - C_B^2\rho g b \\ &- \rho C_a a\frac{(2k)^{1/2}}{L} - \frac{2}{3}k\frac{\partial \rho}{\partial x}\,. \end{aligned} \tag{19}$$

Recall, b is the density-specific-volume correlation. It is defined exactly by $b \equiv -\overline{\rho' v'} = (\overline{\rho})(\overline{v}) - 1$. Let us assume that the mean density profile is given in terms of the density of the heavy fluid, ρ_H, and the density of the light fluid, ρ_L. Then, the self-similar form of the density profile is given by

$$\rho = \rho_0\left(1 + A_T\frac{x}{h}\right)\,, \tag{20}$$

where ρ_0 indicates the density at $x = 0$, and A_T is the conventional Atwood number:

$$\rho_0 = \frac{\rho_H + \rho_L}{2} \quad \text{and} \quad A_T = \frac{\rho_H - \rho_L}{\rho_H + \rho_L}\,. \tag{21}$$

Applying the closure for the mean specific volume used in equation 13 gives the specific volume profile

$$v = \frac{(1+c)\,\rho_0 + A_T\,(c-1)\,\rho_0\left(\frac{x}{h}\right)}{(1+c-A_T^2)\,\rho_0^2 + 2c\rho_0^2 A_T\left(\frac{x}{h}\right) + c\rho_0^2 A_T^2\left(\frac{x}{h}\right)^2}\,. \tag{22}$$

Then, the self-similar form of the density-specific-volume correlation, given in equation 23 can be obtained. To eliminate the x/h dependence in the denominator, it is required that $c = 0$, which reduces the expression further.

$$\begin{aligned} b &= \frac{A_T^2\left[1 - \left(\frac{x}{h}\right)^2\right]}{(1+c-A_T^2) + 2cA_T\frac{x}{h} + cA_T^2\left(\frac{x}{h}\right)^2} \\ &= \frac{A_T^2}{1-A_T^2} f\,. \end{aligned} \tag{23}$$

Let us also define the k-L-a Atwood number,

$$A(x) \equiv \frac{C_A}{1-A_T^2}\frac{L}{\rho_0}\frac{\partial \rho}{\partial x} = C_A\beta\frac{A_T}{1-A_T^2}f^{1/2}\,. \tag{24}$$

Since the self-similar function f has a maximum value of 1 at $x = 0$, it is convenient to define the k-L-a Atwood number such that it has peak value equal to $A_T/\left(1-A_T^2\right)$ at $x = 0$. This constraint requires $C_A = 1/\beta$. The following self-similar form of a is then assumed:

$$\begin{aligned} a &= -C_B A(x)\sqrt{2k} \\ &= -C_B\frac{A_T}{1-A_T^2}\sqrt{2K_0}f\,. \end{aligned} \tag{25}$$

Substituting equations 20, 23, and 25 into equation 19 yields equation 26 after collecting terms and rearranging. For the similarity ansatz to hold, it is required that equation 26 is satisfied for all values of x. The only way this can happen is if both the zero and second moments simultaneously go to zero, which requires $N_a = 2N_L$. Applying this condition reduces both moments to the same result, given by equation 27, where a change of variable has been introduced in terms of the turbulent velocity $V_0 \equiv \sqrt{2K_0}$, and the low-Atwood number approximation has been utilized to drop terms scaling like A_T^2.

$$\underbrace{\left[\frac{\dot{K}_0}{\sqrt{2K_0}}+\frac{C_L N_L}{N_a}\frac{(2K_0)}{L_0}-C_B A_T g+\left(C_a-\frac{\beta\left(1-A_T^2\right)}{3C_B}\right)\frac{2K_0}{L_0}\right]}_{\text{zero moment}}-$$
$$\underbrace{\left[\frac{\dot{K}_0}{\sqrt{2K_0}}+\left(\frac{3C_L N_L}{N_a}-C_L\right)\frac{(2K_0)}{L_0}-C_B A_T g+\left(C_a-\frac{\beta\left(1-A_T^2\right)}{3C_B}\right)\frac{2K_0}{L_0}\right]}_{\text{second moment}}\left(\frac{x^2}{h^2}\right)=0\,. \tag{26}$$

$$\dot{V}_0=C_B A_T g-\frac{V_0^2}{L_0}\left(C_a-\frac{1}{3C_A C_B}+\frac{C_L}{2}\right)\,. \tag{27}$$

C. Self-Similarity of the k Equation

If we again consider the RT-unstable problem in hydrostatic equilibrium, equation 8 may be transformed to the following form of the k equation in one dimension.

$$\frac{Dk}{Dt}=\frac{\partial}{\partial x}\left(\frac{C_\mu L_0 f\sqrt{2K_0}}{N_k}\frac{\partial k}{\partial x}\right)+g\left[C_B\frac{A_T}{1-A_T^2}\sqrt{2K_0}f\right]-C_D\frac{(2k)^{3/2}}{L}\,. \tag{28}$$

After substituting for k, expanding the material derivative, and collecting terms, equation 28 is reduced to a more useful form,

$$\underbrace{\left[\dot{K}_0+\frac{C_L N_L}{2N_k}\frac{(2K_0)^{3/2}}{L_0}-C_B\frac{A_T}{1-A_T^2}g\sqrt{2K_0}+C_D\frac{(2K_0)^{3/2}}{L_0}\right]}_{\text{zero moment}}-$$
$$\underbrace{\left[\dot{K}_0+\left(\frac{3C_L N_L}{2N_k}-\frac{C_L}{2}\right)\frac{(2K_0)^{3/2}}{L_0}-C_B\frac{A_T}{1-A_T^2}g\sqrt{2K_0}+C_D\frac{(2K_0)^{3/2}}{L_0}\right]}_{\text{second moment}}\left(\frac{x}{h}\right)^2=0\,. \tag{29}$$

Following the usual procedure, the zero and second moments must simultaneously to go to zero, which requires $N_k=2N_L$. With this constraint, both moments of the k equation are reduced to a second equation in terms of V_0,

$$\dot{V}_0=C_B A_T g-\frac{V_0^2}{L_0}\left(C_D+\frac{C_L}{4}\right)\,. \tag{30}$$

In order to simultaneously satisfy equations 27 and 30, we require

$$C_a=C_D+\frac{1}{3C_A C_B}-\frac{C_L}{4}\,. \tag{31}$$

D. Richtmyer-Meshkov Growth Rate

Experimental observations are now utilized to provide further constraints. In an RM configuration, after the shock has passed, the acceleration term in equation 30 will vanish. Then substitution of equation 18 into equation 30 gives

$$\frac{2}{C_L}\ddot{L}_0=-2\frac{\dot{L}_0^2}{L_0}\left(\frac{C_D}{C_L}+\frac{1}{4}\right)\,. \tag{32}$$

Integrating this equation for L_0 requires initial values of $L_0(0)$ and $\dot{L}_0(0)$. Anticipating the result, we try a solution of the form

$$L_0(t)=L_0(0)\left[\frac{\dot{L}_0(0)}{\theta L_0(0)}+1\right]^\theta\,. \tag{33}$$

Substituting this equation and its derivatives into equation 32 gives a simple expression, which may be rearranged to provide a constraint on the ratio C_D/C_L in terms of the RM growth rate, θ:

$$\frac{C_D}{C_L} = \frac{2-3\theta}{4\theta}\,. \tag{34}$$

E. Rayleigh-Taylor Growth Rate

In an RT configuration, the acceleration term in equation 30 cannot be dropped. In this case, we assume a solution of the form $L_0 = BA_T g t^2$. Substitution into equation 18 gives $V_0 = \frac{4}{C_L} BA_T g t$. Then, substituting the trial solutions into equation 30 provides a relationship between the RT constant B and the model constants,

$$B = \frac{C_B C_L}{8\left(1+2\frac{C_D}{C_L}\right)}\,. \tag{35}$$

For small Atwood number it is expected that the bubble height will be $h(t)$, and it is expected that bubble height should grow according to $h(t) = \alpha_b g A_T t^2$. Utilizing this relationship, one can derive the following expression for C_B:

$$\begin{aligned} h(t) &= \frac{L_0(t)}{\beta} = \sqrt{\frac{C_\mu C_L}{N_K}}\frac{C_B}{4\left(1+2\frac{C_D}{C_L}\right)} A_T g t^2, \\ C_B &= \frac{4\alpha_b\left(1+2\frac{C_D}{C_L}\right)}{\sqrt{\frac{C_\mu C_L}{N_K}}}\,. \end{aligned} \tag{36}$$

The turbulence kinetic energy generated within an RT mixing layer is given by

$$\begin{aligned} E_K &= \int_{-h}^{h} \rho K(x,t)\mathrm{d}x \\ &= K_0 \int_{-h}^{h} \left(\rho_0 + \frac{\partial \rho}{\partial x} x\right)\left(1-\left(\frac{x}{h}\right)^2\right)\mathrm{d}x \\ &= K_0 \int_{-h}^{h} \left[\rho_0\left(1-\left(\frac{x}{h}\right)^2\right) + \frac{\partial \rho}{\partial x}\left(x - \frac{x^3}{h^2}\right)\right]\mathrm{d}x\,. \end{aligned} \tag{37}$$

By symmetry, the integral over odd powers of x will vanish, leaving $E_K = \frac{4}{3} h(t) \rho_0 K_0(t)$. Since K_0/L_0 is constant, K_0/h should also be constant, which allows further reduction:

$$\frac{K_0}{h} = \beta \frac{K_0}{L_0} = \frac{2\alpha_b A_T g N_K}{C_L C_\mu} \tag{38}$$

and

$$E_K = \frac{8}{3}\left(\frac{N_K}{C_L C_\mu}\right)\alpha_b A_T \rho_0 g h^2\,. \tag{39}$$

The gravitational potential energy within an RT mixing layer can also be derived by imagining a material interface at x=0 and integrating over a distance $2d$,

$$\begin{aligned} \mathrm{PE} &= -g\int_{-d}^{d} \rho(x) x \mathrm{d}x \\ &= -g\int_{-d}^{-h} \rho_L x \mathrm{d}x - g\int_{-h}^{h}\left(\overline{\rho} + \frac{\partial \rho}{\partial x} x\right) x \mathrm{d}x - g\int_{h}^{d} \rho_H x \mathrm{d}x \\ &= -\frac{g}{2}\left(\rho_H - \rho_L\right) d^2 + \frac{g}{6}\left(\rho_H - \rho_L\right) h^2\,. \end{aligned} \tag{40}$$

Since we are only interested in the change in potential energy over the mixing width, we consider the term proportional to h, $\Delta\mathrm{PE} = \frac{g}{6}\left(\rho_H - \rho_L\right) h^2$. Thus, the fraction of potential energy converted to kinetic energy is given by

$$\frac{E_K}{\Delta \mathrm{PE}} = \frac{\frac{8}{3}\frac{N_K}{C_L C_\mu}\alpha_b A_T \frac{\rho_H + \rho_L}{2} g h^2}{\frac{g}{6}\left(\rho_H - \rho_L\right) h^2} = \frac{8 N_K \alpha_b}{C_L C_\mu}\,. \tag{41}$$

F. Self-Similarity of the Scalar Equation

Conservation of species mass fraction in one dimension is given by equation (42), where the species subscript on the mass fraction has been dropped for simplicity,

$$\frac{DY}{Dt} = \frac{\partial}{\partial x}\left(\frac{C_\mu L \sqrt{2k}}{N_Y}\frac{\partial Y}{\partial x}\right)\,. \tag{42}$$

It is assumed that the self-similar solution for the light fluid must look like $Y(x,t) = 0.5\left[1 - x/h(t)\right]$, with derivatives

$$\frac{\partial Y}{\partial t} = \frac{x\dot{h}}{2h^2} \quad \text{and} \quad \frac{\partial Y}{\partial x} = -\frac{1}{2h}\,. \tag{43}$$

It is additionally useful to write

$$\begin{aligned} \sqrt{2k(x,t)} &= \sqrt{2K_0(t)}\sqrt{1-\left(\frac{x}{h}\right)^2} \\ &= \frac{2}{C_L}\dot{L}_0(t)\sqrt{1-\left(\frac{x}{h}\right)^2}\,. \end{aligned} \tag{44}$$

Substituting equations 43 and 44 into equation 42 gives

$$\dot{Y} = \frac{x\dot{h}}{2h^2} = \frac{2C_\mu}{C_L N_Y}\frac{L_0 \dot{L}_0 x}{h^3}\,. \tag{45}$$

Finally, we utilize $L_0 = \beta h$ and $\dot{L}_0 = \beta \dot{h}$ and substitute into equation 45, which gives

$$\dot{Y} = \frac{x\dot{h}}{2h^2} = \frac{N_L}{N_Y}\frac{x\dot{h}}{h^2}\,. \tag{46}$$

Inspection reveals that this equation can only be satisfied if $N_Y = 2N_L$.

TABLE I. Summary of model constants and the equations that constrain them.

	C_μ	C_a	C_B	C_D	C_L	N_a	N_e	N_k	N_L	N_Y	c
Value	0.204	0.339	0.857	0.354	0.283	0.060	0.060	0.060	0.030	0.060	0.000
Equation	-	31	36	54	34	26	51	29	41	45	23

G. Self-Similarity of the Internal Energy Equation

Applying the simplifying assumptions and substituting into equation 7 gives

$$\frac{De}{Dt} = \frac{\partial}{\partial x}\left(\frac{C_\mu L\sqrt{2k}}{N_e}\frac{\partial e}{\partial x}\right) + C_D\frac{(2k)^{3/2}}{L}\,. \tag{47}$$

It is assumed that the self-similar solution takes form $e(x,t) = e_0 + e_1 f(x,t)$. After some algebra and substitution, one obtains

$$\begin{aligned}\frac{e_1 C_L V_0}{L_0}\left(\frac{x}{h}\right)^2 = &-\frac{N_L}{N_e}\frac{e_1 C_L V_0}{L_0}\left[1-3\left(\frac{x}{h}\right)^2\right] \\ &+ C_D\frac{V_0^3}{L_0}\left[1-\left(\frac{x}{h}\right)^2\right]\,.\end{aligned} \tag{48}$$

Again, it is required that the reduced equation must be satisfied for all x, which requires that the zero and second moments must be true simultaneously. We start by considering the zero moment equation,

$$-\frac{N_L}{N_e}\frac{e_1 C_L V_0}{L_0} + C_D\frac{V_0^3}{L_0} = 0 \tag{49}$$

which can be rearranged to give

$$C_D V_0^2 = \frac{e_1 C_L N_L}{N_e}\,. \tag{50}$$

Utilizing equation 50, we can then write the second moment equation,

$$\frac{e_1 C_L V_0}{L_0} = \frac{2N_L}{N_e}\frac{e_1 C_L V_0}{L_0}\,. \tag{51}$$

In order to satisfy the second moment equation, it is required that $N_e = 2N_L$.

H. Decay of Homogeneous Isotropic Turbulence

In the absence of mean velocity or pressure gradients, equations 8 and 9 reduce to ordinary differential equations

$$\frac{dk}{dt} = -C_D\frac{(2k)^{3/2}}{L} \quad \text{and} \quad \frac{dL}{dt} = C_L\sqrt{2k}\,. \tag{52}$$

These equations are solved in terms of a reference time, t_0, and a decay constant, n:

$$k = K_0\left(1+\frac{t}{t_0}\right)^{-n}, \tag{53a}$$

$$L = L_0\left(1+\frac{t}{t_0}\right)^{1-n/2}. \tag{53b}$$

By substituting equations 53a and 53b into equation 52, the following expression is obtained for the decay constant

$$n = \frac{2C_D}{C_L + C_D}. \tag{54}$$

I. Summary of Constraints

To complete the set of model constants, experimental observations are used to set the RT growth rate $\alpha = 0.060$ [10, 11], the RT energetics ratio $E_K/\Delta PE = 0.5$ [11, 12], and the RM growth rate $\theta = 0.25$ [10, 13]. The value for C_μ is something of a free parameter when $C_{dev} = 0$ because its scaling can essentially be accounted for by the diffusion constants N_Y, N_e, N_k, N_L, and N_a; indeed Dimonte and Tipton [1] take $C_\mu \equiv 1$ for this reason. However, in future incarnations of the present model which may include the deviatoric stress tensor, it will be useful to take $C_\mu < 1$ to better account for shear instabilities. In the present work, we take $C_\mu\sqrt{2} = 0.288$ for consistency with experimental RT work by Banerjee *et al.* [14]. The constant C_D is set by the decay of homogeneous isotropic turbulence (HIT), as given by equation 54. Experimental measurements of the decay constant n range between 1.15 and 1.45 [15], while standard k-ϵ [16] and k-L models [1] have historically arrived at lower values of 1.09 and 1.11, respectively. By selecting $C_D = 2^{-3/2} \approx 0.35$, we arrive at a decay constant $n \approx 1.11$. Table I summarizes the complete set of model constants and the equations that constrain them.

A fully constrained model has now been developed that satisfies the ansatz of self-similarity laid out in section III A. It is worth noting, however, that although a particular form of self-similar profiles is assumed, this set is not necessarily the only set that will satisfy self-similarity. Indeed, as a consequence of the assumed profiles, the specific dissipation rate (sometimes referred to as the *turbulent frequency*), ω, should be independent of

space. That is,

$$\frac{k^{1/2}}{L} = \frac{K_0^{1/2}(t) f^{1/2}(\chi)}{L_0(t) f^{1/2}(\chi)} = \omega(t) \, . \tag{55}$$

Although this constraint is close to physical for a range of canonical turbulent flows including grid turbulence, homogeneous shear flows [15], and low-Atwood number Rayleigh-Taylor mixing layers [17], the present model may prove to be too constraining for more complicated flows with spatially varying ω.

IV. COMPUTATIONAL RESULTS

Having derived a set of model constants that satisfy the self-similarity ansatz, it is now desired to apply the model to canonical one-dimensional RT and RM test problems. The *k-L-a* model is implemented in the *Ares* code, which is a second-order arbitrary Lagrangian/Eulerian (ALE) hydrodynamics code developed at Lawrence Livermore National Laboratory (LLNL). In this section, basic units of mass, length, time, and temperature are those used in *Ares*: grams, centimeters, microseconds, and degrees Kelvin.

Self-similar growth is first probed in a simple problem meant to approximate a hydrostatic RT configuration in equilibrium with an acceleration equal to 100 times Earth's gravity. The initial density ρ_0, temperature T_0, and pressure p_0 are summarized by equation 56 in terms of the gas constant R and the acceleration g.

$$\begin{aligned} \rho_0(y) &= \begin{cases} 1.0 & y \geq 0 \\ \frac{1-A_T}{1+A_T} & y < 0 \end{cases}, \\ T_0(y) &= \frac{g}{R} y + 293, \\ p_0(y) &= \rho_0 R T_0 \, . \end{aligned} \tag{56}$$

We consider two ideal, monatomic gases subject to constant acceleration in a unit domain with 1600 uniformly spaced computational volumes, or *zones*. L is initialized to zero everywhere except for the two zones bordering the interface at $y = 0$, where $L = \lambda_0 =$ 4.0e-6. We additionally initialize $k = a_y = 0$ everywhere; however, to ensure production occurs at early time, b is taken as the maximum of 1.0e-4 and the value given by equation 13 in the interface zones. Figure 1 illustrates that excellent self-similar growth is obtained by plotting normalized profiles of k, L, μ_t, a_y, b, and Y_{heavy} against the expected analytic profiles for $A_T = 0.05$. Figure 2 furthermore illustrates that magnitudes of K_0, L_0, and bubble height h_b are well converged, and the bubble growth rate $\alpha_b = h_b / A_T g t^2$ also converges to the model constraint, 0.060. In this case, bubble height is defined at the 99% contour of heavy mass fraction, spike height h_s is defined at the 1% contour, and $h = 0.5(h_b + h_s)$.

Application of the model at higher Atwood numbers is tested in figure 3, which plots normalized profiles of k, L, and a_y for the same RT test problem at $A_T = 0.05$, 0.20, 0.40, 0.60, and 0.80. As the Atwood number is increased, the profiles become offset and skewed towards the spikes, which is consistent with observations made by Dimonte and Tipton[1]; however, the magnitude of the normalized a_y profile is additionally seen to decrease with increasing Atwood number, which might be expected given the Atwood number dependence in equations 23 and 25.

Finally, the *k-L-a* model is applied to the simulation of three different air/SF_6 shock tube experiments ($A_T = 0.67$) to test its ability to predict RM growth rates. In each of the experiments considered [18, 19], a shockwave is driven from air into SF_6 and is reflected. In the Vetter and Sturtevant experiments [19], a rarefaction wave additionally interacts with the mixing zone shortly after the reflected shock. Solutions are found to be well converged for all cases with 2560 zones in the SF_6 test section, 3840 zones of shocked air (157 cm), and 80 zones of ambient air (6.0 cm). An initially diffuse interface of width h_0 is assumed and imposed as initial conditions, as summarized in equation 57. Initial k and a_y are taken to be 0 everywhere.

$$\begin{aligned} Y_{SF_6}(y) &= \frac{1}{2}\left[1 + \tanh\left(\frac{y}{h_0}\right)\right], \\ L(y) &= 4 h_0^{1/2} Y_{SF_6}(y) \left[1 - Y_{SF_6}(y)\right] \, . \end{aligned} \tag{57}$$

As illustrated in figure 4, computed mixing width profiles compare favorably with experiment across a range of Mach numbers. Additionally, it is expected that the mixing width should grow according to $h(t) = h_0 \left[\dot{h}_0 t/(h_0\theta) + 1\right]^{\theta}$. Using this equation, it is possible to fit a curve to the computational profiles after both shock interactions to extract the realized RM growth rate, θ. For the Mach 1.2 case [18], the realized growth rate $\theta \approx 0.251$, which is very close to the model constraint, 0.25. For the higher Mach number cases, $\theta \approx 0.262$, which is consistent with values between 0.258 and 0.264 observed by Dimonte and Tipton [1].

V. SUMMARY

In the present work, an extension of the *k-L* model [1] has been presented in which an additional transport equation is solved for the mass-flux velocity. Detailed similarity analysis was conducted to derive a set of model constants which satisfy an ansatz of self-similarity for RT and RM unstable flows in the limit of low Atwood number. The properly constrained model was then applied to several one-dimensional test problems, and realized growth rates were found to compare favorably with both experiment and the expected theoretical growth rates used to constrain the model. Favorable comparisons with shock tube data up to $A_T = 0.67$ and Mach 1.98 demonstrate model flexibility at least comparable to the standard *k-L* model.

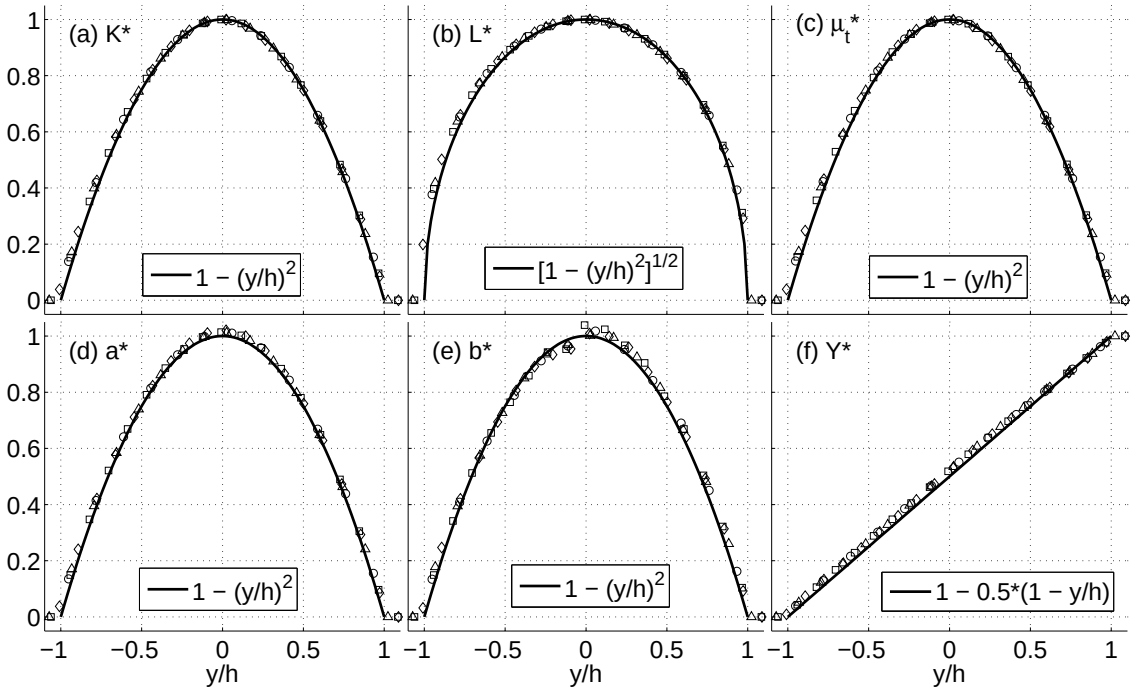

FIG. 1. Normalized profiles obtained for a one-dimensional RT mixing layer of $A_T = 0.05$ at non-dimensional time $\tau = t\,(A_T g/\lambda_0)^{1/2} = 324$ (□), 648 (◯), 972 (△), and 1296 (◇): (*a*) $K^* = k/K_0$, (*b*) $L^* = L/L_0$, (*c*) $\mu_t^* = \mu_t/(C_\mu \rho L_0 \sqrt{2K_0})$, (*d*) $a^* = (A_T^2 - 1)a_y/(C_B A_T \sqrt{2K_0})$, (*e*) $b^* = (1 - A_T^2)b/A_T^2$, and (*f*) $Y^* \equiv$ heavy fluid mass fraction.

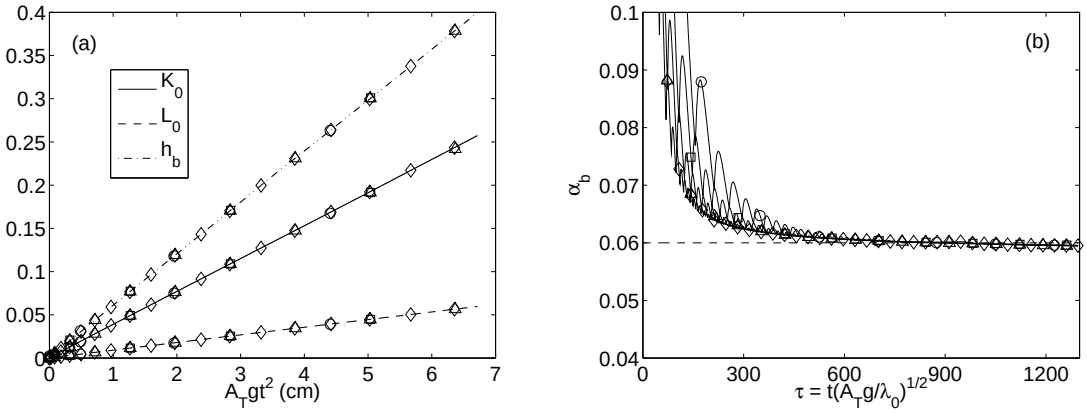

FIG. 2. Convergence of a one-dimensional RT mixing layer at $A_T = 0.05$ with grid resolution of 200 (◯), 400 (□), 800 (△), and 1600 (◇) zones. (*a*) Solutions of h_b, K_0, and L_0. Dimensions are in cm for h_b and L_0 and 10^{-9} $(\mathrm{cm}/\mu\mathrm{s})^2$ for K_0. (*b*) Time history of $\alpha_b = h_b/A_T g t^2$.

Although the present work has focused on validation exercises for which the standard k-L model has already been shown to be effective, the k-L-a model is expected to better capture multi-dimensional turbulent mixing problems which may have significant counter-gradient diffusion, particularly at early time [5]. Further work must be done to apply the k-L-a model to these types of problems, to extend the model to include the effects of the deviatoric stress tensor, and to assess the accuracy of the model when applied to the simulation of turbulent fields with spatially varying specific dissipation rate.

ACKNOWLEDGMENTS

This work was preformed under the auspices of the U.S. Department of Energy by Lawrence Livermore National Laboratory under Contract No. DE-AC52-07NA27344.

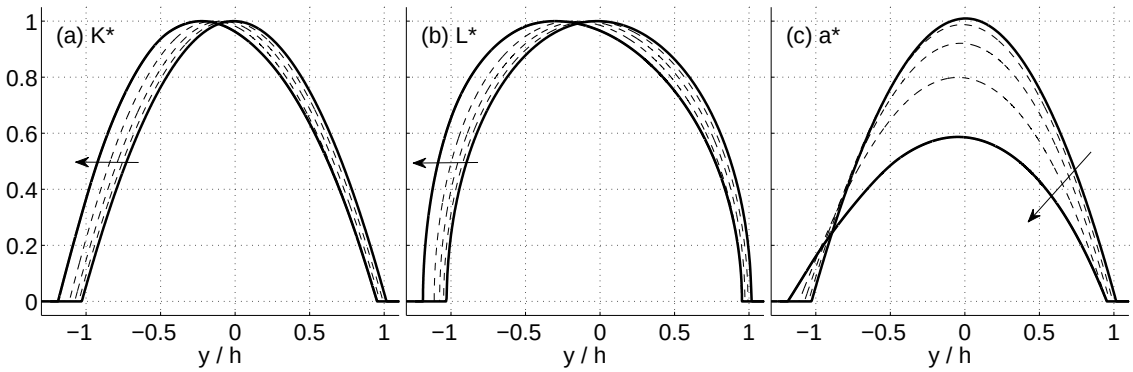

FIG. 3. Normalized profiles obtained for a one-dimensional RT mixing layer of $A_T = 0.05$, 0.20, 0.40, 0.60, and 0.80 at $\tau = t\,(A_T g/\lambda_0)^{1/2} = 1296$: (a) $K^* = k/K_0$, (b) $L^* = L/L_0$, and (c) $a^* = (A_T^2 - 1)a_y/(C_B A_T \sqrt{2K_0})$. Arrows indicate direction of increasing Atwood number.

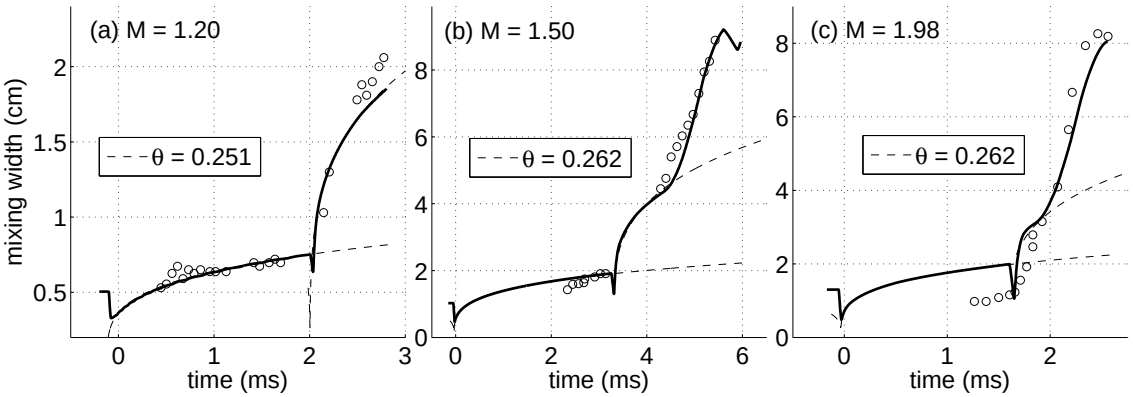

FIG. 4. Mixing width profiles calculated for three different shock tube experiments: (a) Leinov *et al.* experiment 1570 [18] (h_0 = 0.110 cm, test section = 23.5 cm), (b) Vetter and Sturtevant experiment 85 [19] (h_0 = 0.224 cm, test section = 60.0 cm), and (c) Vetter and Sturtevant experiment 87 [19] (h_0 = 0.283 cm, test section = 49.0 cm). Symbols (◯) indicate experimental data. Dashed lines are power law profiles fit to the simulation data.

[1] G. Dimonte and R. Tipton, Phys. Fluids **18**, 085101 (2006).

[2] J. Waltz and T. Gianakon, Computer Physics Communications **183**, 70 (2012).

[3] M. Brüggen, E. Scannapieco, and S. Heinz, Mon. Not. R. Astron. Soc. **395**, 2210 (2009).

[4] V. Smalyuk, O. Hurricane, J. Hansen, G. Langstaff, D. Martinez, H.-S. Park, K. Raman, B. Remington, H. Robey, O. Schilling, R. Wallace, Y. Elbaz, A. Shimony, D. Shvarts, C. D. Stefano, R. Drake, D. Marion, C. Krauland, and C. Kuranz, High Energy Density Physics **9**, 47 (2013).

[5] N. Denissen, B. Rollin, J. Reisner, and M. Andrews, ASME Journal of Fluids Engineering **136**, 91301 (2014).

[6] D. Besnard, F. Harlow, R. Rauenzahn, and C. Zemach, *Turbulence transport equations for variable-density turbulence and their relationship to two-field models*, Tech. Rep. (Los Alamos National Laboratory, 1992).

[7] A. Banerjee, R. Gore, and M. Andrews, Physical Review E **82**, 046309 (2010).

[8] K. Stalsberg-Zarling and R. Gore, *The BHR2 Turbulence Model: Incompressible Isotropic Decay, Rayleigh-Taylor, Kelvin-Helmholtz and Homogeneous Variable Density Turbulence*, Tech. Rep. (Los Alamos National Laboratory, 2011).

[9] K. Sinha, K. Mahesh, and G. Candler, Phys. Fluids **15**, 2290 (2003).

[10] G. Dimonte and M. Schneider, Phys. Fluids **12**, 304 (2000).

[11] G. Dimonte, D. Youngs, A. Dimits, S. Weber, M. Marinak, S. Wunsch, C. Garasi, A. Robinson, M. Andrews, P. Ramaprabhu, A. Calder, B. Fryxell, J. Biello, L. Dursi, P. MacNeice, K. Olson, P. ricker, R. Rosner, F. Timmes, H. Tufo, Y.-N. Young, and M. Zingale, Phys. Fluids **16**, 1668 (2004).

[12] P. Ramaprabhu and M. Andrews, J. Fluid Mech. **502**, 233 (2004).

[13] D. Oron, L. Arazi, D. Kartoon, A. Rikanati, U. Alon,

and D. Shvarts, Phys. Plasmas **8**, 2883 (2001).
[14] A. Banerjee, W. Kraft, and M. Andrews, J. Fluid Mech. **659**, 127 (2010).
[15] S. Pope, *Turbulent Flows*, 5^{th} ed. (Cambridge University Press, Cambridge, UK, 2008).
[16] D. Wilcox, *Turbulence modeling for CFD*, 3rd ed. (DCW Industries, La Cañada, CA, 2010).
[17] J. Ristorcelli and T. Clark, J. Fluid Mech. **507**, 213 (2004).
[18] E. Leinov, G. Malamud, Y. Elbaz, L. Levin, G. Ben-Dor, D. Shvarts, and O. Sadot, J. Fluid Mech. **626**, 449 (2009).
[19] M. Vetter and B. Sturtevant, Shock Waves **4**, 247 (1995).